MOLECULAR AND CELLULAR BIOLOGY, Apr. 2003, p. 2709–2719 Vol. 23, No. 8
0270-7306/03/$08.00+0 DOI: 10.1128/MCB.23.8.2709–2719.2003

Endogenous Assays of DNA Methyltransferases: Evidence for Differential Activities of DNMT1, DNMT2, and DNMT3 in Mammalian Cells In Vivo

Kui Liu, Yun Fei Wang, Carmen Cantemir, and Mark T. Muller*

Department of Molecular Genetics, Ohio State University, Columbus, Ohio 43210

Received 17 December 2002/Accepted 14 January 2003

While CpG methylation can be readily analyzed at the DNA sequence level in wild-type and mutant cells, the actual DNA (cytosine-5) methyltransferases (DNMTs) responsible for in vivo methylation on genomic DNA are less tractable. We used an antibody-based method to identify specific endogenous DNMTs (DNMT1, DNMT1b, DNMT2, DNMT3a, and DNMT3b) that stably and selectively bind to genomic DNA containing 5-aza-2′-deoxycytidine (aza-dC) in vivo. Selective binding to aza-dC-containing DNA suggests that the engaged DNMT is catalytically active in the cell. DNMT1b is a splice variant of the predominant maintenance activity DNMT1, while DNMT2 is a well-conserved protein with homologs in plants, yeast, *Drosophila*, humans, and mice. Despite the presence of motifs essential for transmethylation activity, catalytic activity of DNMT2 has never been reported. The data here suggest that DNMT2 is active in vivo when the endogenous genome is the target, both in human and mouse cell lines. We quantified relative global genomic activity of DNMT1, -2, -3a, and -3b in a mouse teratocarcinoma cell line. DNMT1 and -3b displayed the greatest in vivo binding avidity for aza-dC-containing genomic DNA in these cells. This study demonstrates that individual DNMTs can be tracked and that their binding to genomic DNA can be quantified in mammalian cells in vivo. The different DNMTs display a wide spectrum of genomic DNA-directed activity. The use of an antibody-based tracking method will allow specific DNMTs and their DNA targets to be recovered and analyzed in a physiological setting in chromatin.

In eukaryotes, DNA methylation is an epigenetic encryption system that is essential for proper gene regulation (for reviews see references 2, 4, 7, 23, 29, and 30). Defects in methylation lead to diverse disorders from mental retardation to immune deficiencies, and there is particularly strong evidence that methylation defects create a favorable environment for malignant transformation (2, 3). Pharmacologic alterations in methylation of specific genes have also been correlated with tumor response to chemotherapy and patient survival; thus, methylation regulation and the enzymes that catalyze the process represent important areas for treating cancer (2, 30).

The enzymatic machinery that mediates methylation involves a number of DNA (cytosine-5) methyltransferase (DNMT) isoforms, including DNMT1, DNMT1b, DNMT2, DNMT3a, and DNMT3b (and a host of DNMT3 splice variants) (4, 29, 30). *Dnmt1*, *Dnmt3a*, and *Dnmt3b* are independent genes and essential; embryos lacking both copies of *Dnmt1* or *Dnmt3b* die before birth, whereas *Dnmt3a*-nulls survive about 4 weeks (18, 21). Heterozygous mutants appear normal and are fertile (18, 21). The murine DNMT3a and -3b enzymes appear to possess de novo methylation activity (based upon plasmid methylation), and there is evidence that they act on different DNA targets in vivo (12). No transmethylase activity has been found with DNMT2, and biallelic deletions appear to possess normal methylation patterns (8, 22). How different DNMTs are directed to specific sites in vivo is not well understood, although DNA sequence, chromatin structure, or ancillary interacting factors (or a combination of these) are obvious candidates. In order to sort out which specific DNMTs are responsible for methylation of selected DNA targets, one needs to examine individual methylases in vivo under physiological conditions. Achieving this objective is complicated when one considers that the most prevalent methylase is DNMT1, with DNMT3a and -3b being barely detectable (31), while there exist additional minor forms, including DNMT2 and DNMTb (5, 8, 13, 22). Recently, a cell line knockout of *Dnmt1* was characterized (28) that displayed nearly normal global genomic methylation. Other methylases must be active in this case. For example, DNMT3b is thought to be the additional activity that cooperates with DNMT1 to maintain cellular DNA methylation patterns (28). Additional minor but active DNMTs that are physiologically relevant exist (8, 13, 22). Minor methylating activities may be less robust overall (relative to DNMT1) but have important consequences if key regulatory genes are their targets.

We have developed a method to facilitate elucidation of the methylation machinery that acts in a chromosomal setting. The approach is based on studies showing that DNA methyltransferases have a fleeting covalent association with the DNA substrate; however, when 5-aza-2′-deoxycytidine (aza-dC) is present, the covalent DNA-protein intermediate is arrested, leading to adducts that have consequences in global methylation (9, 15, 33, 34). Consequently, active methylases become stoichiometrically removed from the active nuclear pool, leading to hypomethylation of the genome. We have used an antibody-based method to detect and quantify the physical inter-

* Corresponding author. Mailing address: Department of Molecular Genetics, Ohio State University, 484 West 12th Ave., Columbus, OH 43210. Phone: (614) 292-1914. Fax: (614) 292-4702. E-mail: muller.2@osu.edu.

action of several different DNMTs on the genome of the cell in vivo.

MATERIALS AND METHODS

Reagents. The topoisomerase I (topo I) antibody was isolated from serum of scleroderma patients and was donated by TopoGEN, Inc. (www.topogen.com) (Columbus, Ohio). Anti-DNMT1 rabbit antibody was prepared by using a commercial antibody production service (Research Genetics) and was raised against a synthetic peptide derived from the N-terminal region. Anti-DNMT1b rabbit antibody was prepared against a peptide unique to the additional exon not present in DNMT1 (5, 13). All peptide antibodies were immunoaffinity purified and tested by enzyme-linked immunosorbent assay and Western blotting for appropriate reactivity. Anti-DNMT2 antibody prepared against DNMT2 was provided by X. Cheng and Anti-DNMT3a and -3b antibodies (specific for mouse DNMT3) were provided by K. Robertson. All DNMT antisera were verified for specificity by Western blotting by using crude extracts. Camptothecin (CPT) and etoposide (VP16) were provided by TopoGEN, (in 100% dimethyl sulfoxide), and aza-dC was from Sigma Chemical Co. (St. Louis, Mo.). aza-dC was prepared fresh just prior to use.

Cell culture. HeLa, WI-38, HCT-116 (wild type), and HCT-116 *Dnmt1*$^{-/-}$ (27) cell lines in this study were cultured in Dulbecco's modified Eagle medium supplemented with 10% fetal bovine serum (CellGro, Inc., Herndon, Va.). Jurkat cells were grown in RPMI medium supplemented with 10% fetal bovine serum. HCT-116 cells were kindly supplied by B. Vogelstein and S. Baylin. Mouse teratocarcinoma cell line P19 was provided by K. Robertson. Cells were grown in a humidified atmosphere of 5% CO_2–95% air at 37°C.

Nuclear protein preparation, band depletions, and Western blotting analysis. To prepare samples for Western blotting, cells were washed twice with cold phosphate-buffered saline and resuspended in 1 ml of buffer A (100 mM NaCl, 50 mM KCl, 20 mM Tris-HCl, pH 7.5, 0.1 mM EDTA, 0.1 mM phenylmethylsulfonyl fluoride, 10% glycerol, 0.2% NP-40, and 0.1% Triton X-100). Following incubation on ice (10 min), nuclei were centrifuged (2,000 × *g*, 10 min) and lysed in 100 μl of 1× electrophoresis sample buffer and boiled for 2 to 3 min. The samples were separated by gradient sodium dodecyl sulfate (SDS)-polyacrylamide gel electrophoresis, followed by electroblot transfer to nitrocellulose. Immune complexes were illuminated by using the BM Chemiluminescence Western blotting kit (mouse/rabbit) (Boehringer Mannheim GmbH, Mannheim, Germany) as described previously (20).

ICM analysis. The method for detecting DNMT-genomic DNA adducts is based upon technology developed to measure topoisomerase-DNA adducts (36) (Fig. 1C). Cells were treated with aza-dC as specified by each experiment. It is essential that negative controls (no drug treatment) be included in each analysis. Typically 1×10^7 to 5×10^7 cells were used for each ICM analysis (a single 100-mm dish, although the method works equally well with adherent and nonadherent cells). Following drug treatment, the medium was removed by suction and the cells were lysed by immediate addition at 37°C of 1% Sarkosyl in Tris-EDTA (TE) (10 mM Tris-HCl, pH 7.5, 1 mM EDTA). For a 100-mm petri dish, 2 ml of Sarkosyl lysis solution was used; the plates were swirled several times to promote complete dispersion and lysis of the monolayer. For Jurkat (suspension) cells, the cells were deposited by centrifugation, the supernatant were decanted and cells were lysed with 3 ml of 1% Sarkosyl–TE as described above. The lysate was then gently sheared (18-gauge needle) and layered onto a step CsCl gradient made in a Beckman SW41 polyallomer centrifuge tube (14 by 89 mm). The gradients are composed of four layers (2 ml each) of different densities of CsCl made in TE as follows: a stock solution of CsCl was made fresh by dissolving 120 g of CsCl in 70 ml of sterile TE (final density of 1.86 g/ml; refractive index of 1.414). From this stock, four solutions (A to D) were prepared as follows: solution A, 0.075 volumes of TE plus 0.925 volumes of CsCl stock; solution B, 0.2 volumes of TE plus 0.8 volumes of CsCl stock, solution C, 0.45 volumes of TE plus 0.55 volumes of CsCl stock, and solution D, 0.55 volumes of TE plus 0.45 volumes of CsCl stock. By using a 5-ml pipette, 2 ml each of solutions A, B, C, and D from bottom to top of tube was layered. The lysates were overlaid onto step gradients that were topped and balanced with mineral oil followed by centrifugation (30,000 rpm for 20 h at 20°C with a Beckman SW41 rotor). The gradient was fractionated into 0.4-ml aliquots by piercing the bottom of the tube. The DNA peak, which comes out near the bottom of the tube, is easily identified by notable increases in viscosity. To accurately locate DNA-containing fractions, 30 μl of each fraction is diluted into 270 μl of water and absorbance is measured at 260 nm. Peak fractions were pooled, and the DNA concentration was accurately measured by either fluorometry or UV spectroscopy. The DNA pools can be stored indefinitely at −20°C. DNA concentrations were all adjusted to equivalence and were verified by loading a fixed amount

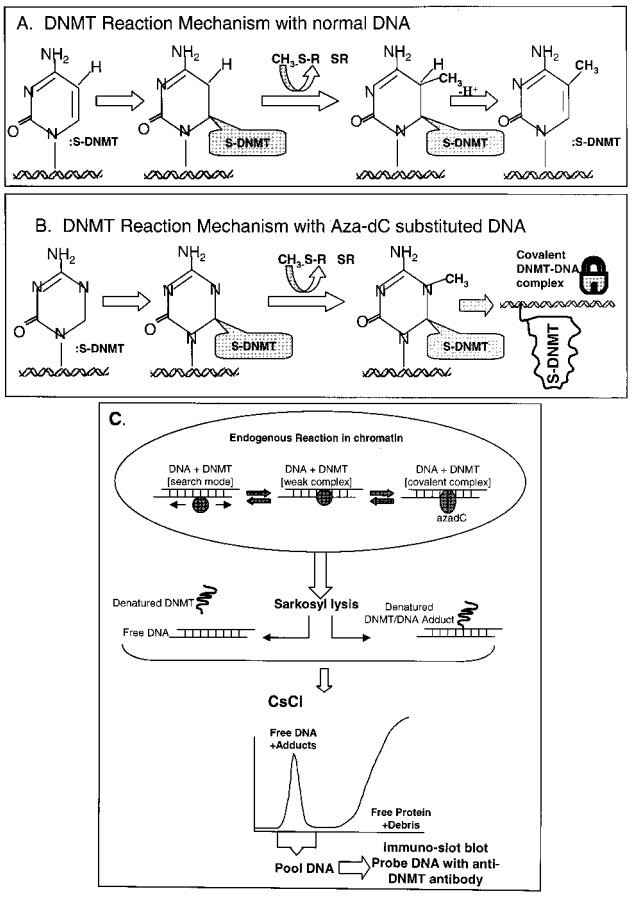

FIG. 1. DNMT reaction mechanism and the ICM assay. (A) Methylation on non-aza-dC-containing DNA proceeds via a nucleophilic attack by cysteine thiolate of DNMT at the C-6 on cytosine followed by a second nucleophilic attack at C-5 by the methyl group of *S*-adenosylmethionine (methyl donor). This results in the transfer of the methyl group to C-5 and an intermediate that is resolved by β elimination of DNMT at C-6 and abstraction of a proton from C-5. (B) Mechanism of action on aza-dC-substituted DNA involves a methyl transfer at the N-5 of aza-dC and formation of a stable or covalent complex between enzyme and DNA that is resistant to ionic detergents, high ionic strength, and temperature (viz., conditions that dissociate proteins that are noncovalently bound to DNA) (9, 10, 15, 34). (C) Overview of the ICM assay. The endogenous DNMT reaction in vivo shows the enzyme in either a one-dimensional search mode (scanning for suitable CpG targets in chromatin) in a weak binding mode (enzyme paused over a chromatin-accessible CpG site in vivo) or in the covalent DNMT-DNA complex mode with aza-dC-substituted DNA. Direct addition of Sarkosyl lyses the cells and disrupts weak (noncovalent) protein-DNA complexes in chromatin; however, aza-dC-induced DNMT-DNA complexes are not dissociable under these conditions. The viscous lysate is sheared and overlaid onto a step CsCl gradient (Materials and Methods) that resolves DNA from the bulk, excess free protein and debris in a single step (35, 38, 39). Proteins stably bound to the DNA are dragged down to the 1.7-g/ml fraction of the gradient. The DNA fraction contains DNMTs only when the cells have been prelabeled with aza-dC. Specific DNMTs are quantified in the DNA peak by Western slot blotting. Note that the material at the top of the gradient gives a nonspecific Western blot signal due to the excess of membranous debris and cannot be relied on to measure free DNMT. To demonstrate that the DNA peak-associated DNMT signal is real (and not carryover from the top of the gradient), the DNA peak can be collected and rebanded in CsCl to give quantitative recovery of the DNMT signal in a second gradient (data not shown). The ICM data were not affected by digestion of lysates with RNase A prior to centrifugation; therefore, RNase digestion was deemed unnecessary.

(from 50 to 200 ng of each DNA sample) onto a 1% agarose gel, followed by electrophoresis (150 V for 10 min) and staining with 0.5 μg of ethidium bromide/ml (30 min) and destaining with water for 15 min. Gels were photographed and band intensities were compared between samples to verify that DNA concentrations were identical.

Immunodetection of proteins in the DNA peak. Immunoblotting with a standard slot blot manifold (Schleicher & Schuell, Keene, N.H.) was carried out on the DNA pool from each gradient as follows: Hybond enhanced chemiluminescence nitrocellulose membranes (cut to fit a slot blot manifold) were soaked for 15 min in 25 mM sodium phosphate buffer, pH 6.5, at room temperature. The slot blot manifold was assembled by placing two pieces of Whatman no. 1 filter paper under the nitrocellulose membrane. The viscosity of the DNA was reduced by shearing with a 21- or 25-gauge needle and a 1-ml syringe. The DNA samples (typically from 20 to 100 μl) were diluted with an equal volume of 25 mM sodium phosphate buffer (pH 6.5) and were applied to the slot blot device under vacuum until all traces of liquid were drawn down. The membrane was removed from the manifold and was immediately immersed in 25 mM phosphate buffer, pH 6.5, for 5 min at room temperature. Membranes were then equilibrated in Tris-buffered saline–Tween (TBST) (20 mM Tris-HCl, pH 7.5, 137 mM NaCl, 0.1% Tween 20) for 15 min with gentle agitation, followed by blocking with TBST containing 5% nonfat dried milk for 2 to 3 h at room temperature. The blots were then washed three times with TBST for 10 min each at room temperature. The primary antibody was diluted as appropriate (1:1,000 to 1:10,000) in 10 to 50 ml of TBST. Blots were incubated with primary antibody for 6 h at room temperature, followed by washing three or four times with TBST (10 min per wash, with gentle agitation). The blots were processed to illuminate the immune complexes in either of two ways. In the first method, the nitrocellulose membranes were incubated with in 30 ml of TBST containing 0.4 μCi of ^{125}I-protein A/ml for 2 h at room temperature. Following several washes with TBST (10 min each, with agitation at room temperature), the membranes were air dried, wrapped in Saran Wrap, and visualized by autoradiography. The second method involved visualization of complexes by chemiluminescence with Amersham's enhanced chemiluminescence kit. The primary antibody incubation step was for 1 h at room temperature, followed by three TBST washes as described above. The blots were incubated with horseradish peroxidase-conjugated secondary antibody for 30 min at room temperature and washed four times in TBST, followed by detection as per the kit protocol. Blot signals were quantified by either densitometry of autoradiograms or on a phosphorimager, and results were expressed as arbitrary signals per microgram of DNA. All ICM data were verified by three independent experiments.

RESULTS

The ICM technique. We have developed an in vivo assay that measures the physical interaction between DNMT and the genome (ICM assay for in vivo complex of methylase). The ICM assay is based upon known details about the reaction mechanism of this class of enzymes (15, 34), and it was previously demonstrated that DNMT1-DNA adducts survive harsh conditions of high salt and detergent (9). The enzyme engages DNA in an intermediate complex where the DNA (at a target cytosine) is covalently linked to the methyltransferase. This covalent intermediate is transient and is released in the last step of the reaction sequence. The interaction of DNMT with the 5-aza-substituted cytosine in DNA (in the presence of *S*-adenosylmethionine) results in formation of an irreversible protein-genomic DNA adduct. Essentially, the catalytic center of DNMT becomes covalently bound to the 6 position of cytosine (Fig. 1A and B). An overview of the ICM assay is shown in Fig. 1C. To validate the specificity and resolving power of the ICM technique, we focused initially on the predominant DNA methylation activity, DNMT1, by using a peptide antibody prepared against the amino terminus of DNMT1 that does not share homology with other DNMTs (for other than DNMT1b, see below and Materials and Methods). The results (Fig. 2A) clearly show that, in the presence of aza-dC, a strong DNMT1 signal was detected in the DNA peak (row 1). The DNMT1 signal in the DNA fraction required aza-dC (compare rows 1 and 2 [Fig. 2A]). The ability of the anti-DNMT1 antibody to detect a specific polypeptide on Western blots is shown in Fig. 2B (lane 2).

In order to determine whether the entire DNMT1 signal in the DNA peak off CsCl was physically bound to DNA and to ensure that essentially all DNMT in the DNA peak is attached to DNA, the following experiments were carried out: DNA was recovered from aza-dC-treated cells and digested exhaustively with DNase I. DNMT1 was then evaluated for electrophoretic mobility shifting on Western blots before and after digestion (Fig. 2C). Prior to digestion (Fig. 2C, lane 2), little if any distinct DNMT1 signal was visible; however, after DNase I, a strong band appeared (Fig. 2C, lane 3), which was shifted to a higher molecular weight (relative to free DNMT1 in a nuclear extract [Fig. 2C, lane 1]). The molecular mass increase (estimated to be 8 to 10 kDa) corresponds to roughly 20 to 30 nucleotides of DNA stably bound to DNMT1. These results show that any DNMT1 signal in the DNA peak is bound to genomic DNA. An independent verification of this idea comes from the following experiment: the DNA peak from aza-dC-treated cells was pooled, dialyzed, and rerun on a second CsCl gradient. The DNMT1 signal in the DNA fraction was quantitatively recovered (data not shown). From these experiments we conclude that DNMT1 is present in the DNA fraction due to its association with genomic DNA and not to adventitious trapping or cross contamination with the free DNMT1 present at the top of the gradient. Since the complexes survive through two rounds of centrifugation (48 h), we conclude that they are not reversing at least over this time period.

To examine specificity and efficiency of the ICM assay for detecting a specific DNMT isoform, additional experiments were required. First, we analyzed mutant and wild-type HCT-116 cells for "band depletion" of DNMT1 on Western blots. WI-38 (control cells) and wild-type HCT-116 cells show the presence of DNMT1 at its expected molecular weight (Fig. 2D); however, the polypeptide signal is reduced substantially after exposure to aza-dC due to the binding of DNMT1 to the genomic DNA (it is band depleted in this case; compare lanes 3 and 4 and lanes 5 and 6 in Fig. 2D). The degree to which the band is depleted in this analysis reflects the efficiency of trapping of DNMT1 on the genome of the cell. These data show that 75 to 80% of the DNMT1 in the cell is lost after aza-dC treatment in this experiment. The fact that a normal cell line (WI-38 diploid fibroblasts) and a tumor cell line (HCT-116) both displayed this high degree of efficiency demonstrates that the ICM efficiency is consistent in cells with diverse growth phenotypes. An additional control using a mutant HCT-116 cell line lacking both copies of DNMT1 (27) confirms that the signal detected (filled arrow [Fig. 2D]) is indeed the DNMT1 polypeptide (it is missing in the mutant). Moreover, aza-dC treatment of the mutant cell line had no effect on the polypeptide profile (Fig. 2D, lanes 1 and 2). Second, ICM results on the HCT-116 wild type and *Dnmt1*$^{-/-}$ mutants (Fig. 2E) are mutually consistent with the band depletion data. These data reveal that in *Dnmt1*$^{-/-}$ mutant cells the antibody did not detect any DNMT1 in the DNA peak (even after aza-dC treatment). DNMT1 protein was detected only in the wild-type HCT-116 cells prelabeled with aza-dC.

Since slot blotting is not based upon molecular weight (relies

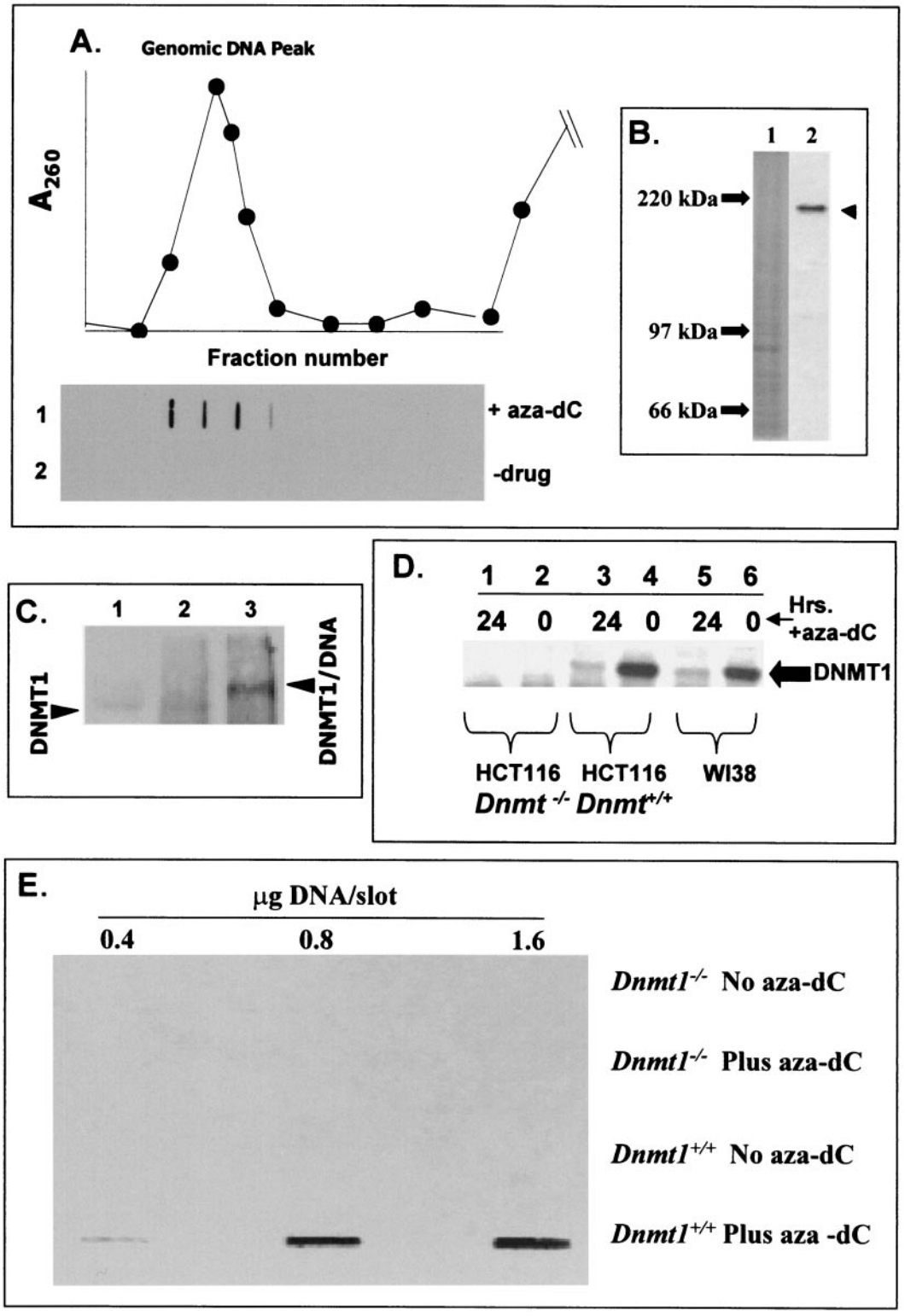

FIG. 2. ICM and band depletion analysis of *Dnmt1*$^{-/-}$ and *Dnmt1*$^{+/+}$ HCT-116 colon cancer cells with and without aza-dC. (A) ICM assay results with HeLa cells. Approximately 3×10^7 HeLa cells in exponential growth were untreated or treated with 5 μM aza-dC for 24 h; following Sarkosyl lysis, the DNA was banded in CsCl, the gradient was fractionated, and the DNA peak was located by UV absorbance. Individual fractions were slot blotted onto membranes and probed with anti-DNMT1 antibody as described in Materials and Methods. Each slot corresponds to the gradient fraction shown in the graph (top fractions of gradient not shown). (B) Western blotting of DNMT1 in HeLa cell extracts. Nuclear extracts (100 μg) were subjected to SDS-polyacrylamide gel electrophoresis, and the Western blots were probed with anti-DNMT1 antibody as described in Materials and Methods. Lane 1, stained gel (molecular weight markers indicated); and lane 2, autoradiogram. (C) Electrophoretic mobility shifts. HeLa cells were treated with aza-dC exactly as described for panel A and were subjected to ICM. The DNA was recovered and dialyzed

on antibody specificity), it is important to show that covalent binding of a heterologous protein to genomic DNA does not generate a signal in the DNA peak when probed with anti-DNMT1 antibody. We utilized topoisomerase poisons to examine this possibility. Exponentially growing HeLa Cells were first incubated with aza-dC, and the cells were then pulsed with a topo II drug (VP16) or a topo I drug (CPT) for 30 min prior to harvest. These conditions promote covalent trapping of topo II or topo I on genomic DNA (37). Western probing of the ICM Western blot with anti-DNMT1 probe from cells treated with VP16 or CPT but not exposed to aza-dC (Fig. 3A) gave no detectable signal. This control demonstrates specificity of the ICM, since these conditions clearly promote topo-DNA complexes (compare Fig. 3C; data for topo II antibody probe not shown). As expected, combining VP16/aza-dC or CPT/aza-dC also yielded a positive DNMT1 signal in the DNA peak (Fig. 3B). Short exposure to CPT elevated DNMT1-DNA complexes by about 25 to 30% (compare aza-dC and CPT and aza-dC alone [Fig. 3B]). The effect was not large but was reproducible (four experiments) and was not seen in aza-dC/VP16 (topo II)-treated cells.

Kinetics of complex formation with different DNMT isoforms. The time course of DNMT1 complex formation was analyzed by the ICM in exponentially growing HeLa cells (Fig. 4A). At the shortest time tested (2.5 h), the highest level of complex formation was detected (two- to threefold greater than later time points); however, complexes stabilized at a fixed but lower level over a period of 73 h. In a variety of human and mouse cell lines tested, DNMT1 complexes formed rapidly (within 10 min, earliest time tested, not shown) and were subsequently (usually within 6 h) reduced to basal, stable levels as depicted in Fig. 4B with Jurkat cells.

Endogenous covalent DNA binding of different DNMTs can be analyzed by using the ICM technique with the appropriate antibodies. The splice variant DNMT1b has been identified as a minor methylase activity in vitro (5, 13). We used the ICM to examine whether this enzyme is an endogenous, functional methylase that targets the genome. DNMT1b differs from DNMT1 by the addition of 16 amino acid residues (between exons 4 and 5). We raised a peptide antibody to this 16-amino-acid region and used it to probe Western blots from an ICM analysis (Fig. 5). Since the 16 amino acids are unique to DNMT1b, this antibody detects only the splice variant, even in the presence of excess DNMT1. The rate of complex accumulation was essentially identical for both DNMT1 isoforms; however, DNMT1b represents about 10% (±3% in repeat experiments) of DNMT1 complex yield. Complex formation was maximal for both isoforms at drug concentrations in the 1 to 10 μM range (data not shown). As expected, we did not detect DNMT1b by using the ICM on *Dnmt1*$^{-/-}$ biallelic knockout deletions (data not shown).

DNMT2 is a well-conserved enzyme of both eukaryotes and prokaryotes; however, despite the presence of a number of sequence motifs common to active DNMTs, this isoform has not been shown to possess in vitro activity (8), nor is it essential for de novo or maintenance methylation events in embryonic stem cells (22). We examined DNMT2 activity in HeLa cells by using the ICM assay. When the ICM blots were probed with anti-DNMT2 antibody (8), we found an aza-dC-dependent signal associated with genomic DNA (Fig. 5). The signal was much weaker than that of DNMT1 (ca. 5%). The time course of DNMT2-DNA adduct formation was very different from that of DNMT1 and -1b isoforms, suggesting that the former activity is regulated independent from the known maintenance activities. The data show that DNMT1, -1b, and -2 are differentially trapped on aza-dC-labeled genomic DNA.

The availability of well-characterized antibodies to mouse DNMTs allowed us to compare DNMT isoforms in a single cell line (mouse teratocarcinoma cell line P19). We compared DNMT1, DNMT2, DNMT3a, and DNMT3b in P19 cells treated with different concentrations of aza-dC (Fig. 6A). ICM analyses were carried out on all four different DNMTs by using the appropriate antibody probes. We selected a time after aza-dC addition when the complex formation had stabilized (8 h [Fig. 5]). Western blot experiments evaluated each DNMT isoform to demonstrate antibody specificity (except for DNMT1, which is shown in Fig. 2B). Westerns blots were also compared from aza-dC-treated and untreated cells for DNMT2, -3a, and -3b (Fig. 6A) to evaluate the efficiency of adduct formation with these different isoforms. (As noted above, substantial band depletion was seen with DNMT1 following aza-dC [Fig. 2D] treatment, suggesting that the efficiency of adduct formation was greater than 75%.) In parallel, complex formation was measured by the ICM assay (at fixed genomic DNA concentrations indicated in Fig. 6 and with increasing amounts of aza-dC). Quantitation of DNMT-DNA complexes based on band depletion was difficult, although we note that, for the three DNMTs tested, it appears that signals were slightly reduced by aza-dC; thus, complex formation was much less efficient (estimated to be 10%) for these DNMTs than for DNMT1 (Fig. 2D). We note however that all isoforms were still detected by the ICM assay. ICM data revealed that DNMT2 and DNMT3a complex formation was roughly three- to fivefold lower than that of DNMT3b (at 8 h after drug addition). DNMT1 complexes were the most abundant of all, as noted with HeLa cells (note that 10-fold less DNA was

against TNM (10 mM Tris-HCl, pH 8.0, 1 mM EDTA, and 10 mM $MgCl_2$), and aliquots were removed for digestion with 50 μg of DNase I/ml (60 min at 37°C). DNA was immunoprecipitated with anti-DNMT1 antibody and was analyzed by SDS-polyacrylamide gel electrophoresis followed by Western blotting (probed with anti-DNMT1 antibody). Lane 1, HeLa nuclear extract control showing the position of DNMT1 polypeptide from non-drug-treated cells. Lane 2, anti-DNMT1 immunoprecipitated DNA (from CsCl gradient) before DNase I digestion. Lane 3, same as lane 2, after DNase I digestion. (D) Band depletion analysis of DNMT1 in *Dnmt1*$^{+/+}$ and *Dnmt1*$^{-/-}$ HCT-116 and WI-38 cell lines. Cells (10^7/dish) were exponentially growing when treated (or not as indicated on the top of the blot) with 5 μM aza-dC for 12 h at 37°C in tissue culture medium plus 10% bovine calf serum. Nuclear proteins were extracted for SDS-polyacrylamide gel electrophoresis and Western blotting as described in Materials and Methods by using anti-DNMT1 antibody probe. The large filled arrow marks the position of the DNMT1 polypeptide band. (E) ICM analysis of DNMT1 in HCT-116 *Dnmt1*$^{+/+}$ and *Dnmt1*$^{-/-}$ cells. Cells were treated with aza-dC or untreated as described for panel D above and were subjected to the ICM analysis. The DNA peak was pooled, and its concentration was measured. Either 0.4, 0.8, or 1.6 μg of DNA was slot blotted onto a membrane, which was probed with DNMT1 antibody.

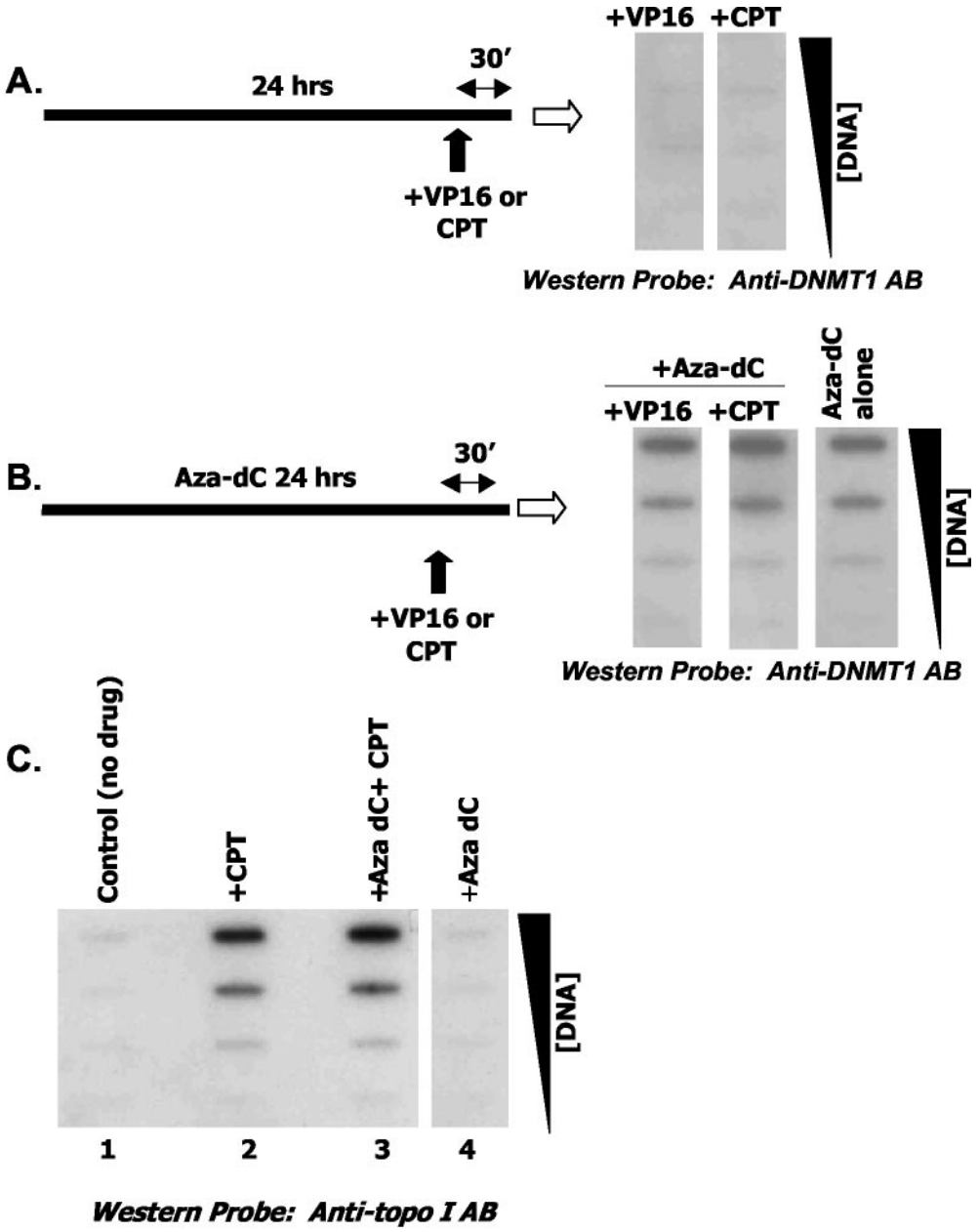

FIG. 3. Combined effects of topo I and II trapping on DNMT1 adduct formation. HeLa cells (exponentially growing; 4×10^7 cells/ICM) were cultured for 24 h without or with aza-dC (5 μM), followed by 30 min of exposure to VP16 (10 μM) or CPT (50 μM) as indicated and subjected to the ICM assay. Increasing amounts of DNA (from 1 to 10 μg) were spotted on the membrane. (A) Two cultures were treated with either VP16 or CPT and probed with anti-DNMT1 antibody. (B) Three plates were treated with aza-dC alone or with aza-dC/VP16 and aza-dC/CPT as indicated. Increasing amounts of DNA were spotted and probed with anti-DNMT1 antibody. Panel C shows several controls where the blot was probed with anti-topo I antibody.

loaded for DNMT1 than for the others in the ICM data shown in Fig. 6). DNMT3a complexes were clearly less common than those of DNMT3b. The differences between DNMT2, -3a, and -3b complexes (by ICM) are not reflected at the polypeptide level. In Fig. 6B, extracts were probed with a mixture of antisera to get an idea of the relative amount of each isoform in the same extract. DNMT2 and -3a were similar, while less DNMT3b was detected. These data suggest that P19 cells possess catalytically active DNMT1, -2, -3a, and -3b, with DNMT1 and -3b having the greatest amount of methylation activity directed at the endogenous genome.

DISCUSSION

The ICM assay is based on known details about the reaction mechanism of this class of enzymes where a putative covalent complex forms between the target cytosine and DNA methyltransferase (9, 15, 33, 34). Under normal circumstances, the

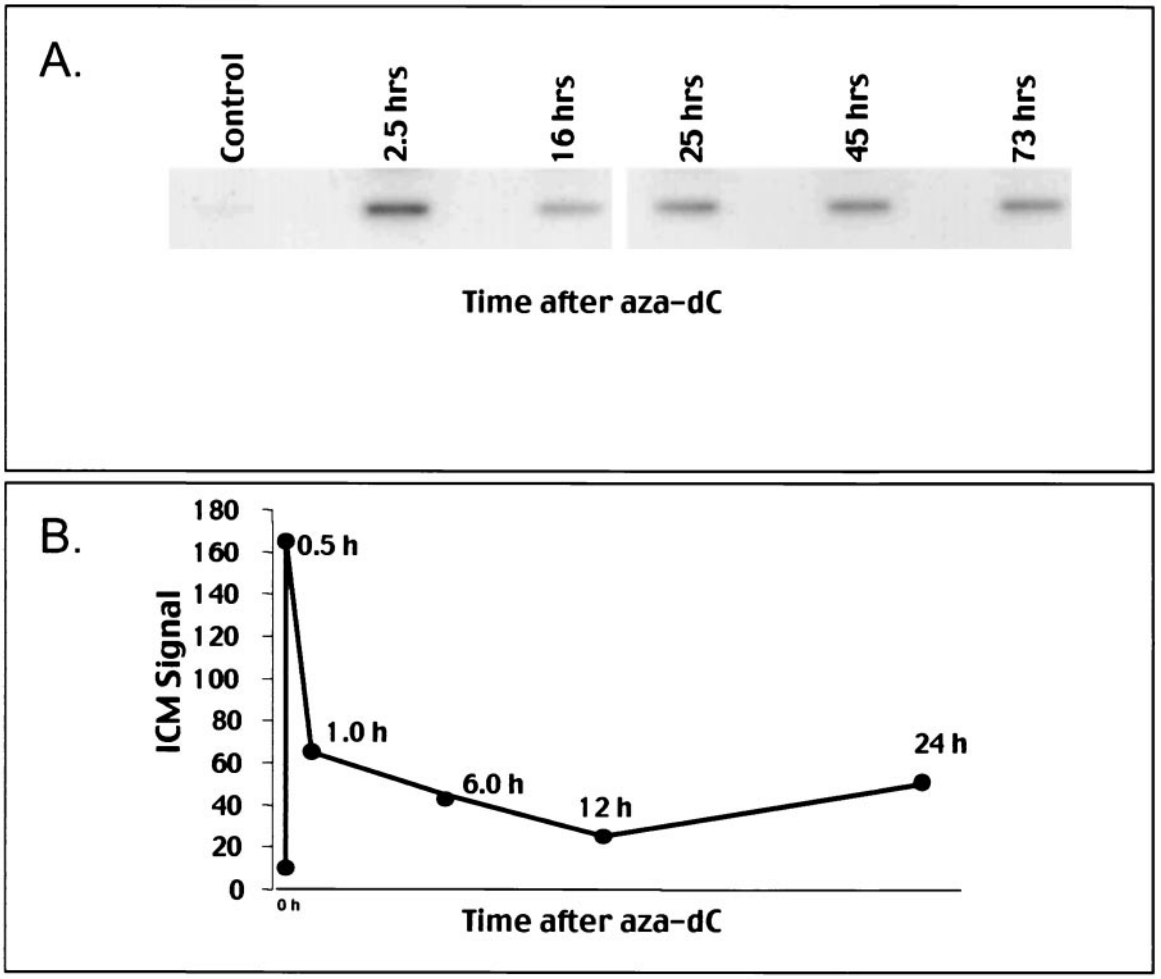

FIG. 4. ICM time course and aza-dC dose response in different cell lines. (A and B) Time course of DNMT1 adduct formation. HeLa cells (A) or Jurkat cells (B) in exponential growth were treated with 5 μM aza-dC or untreated. Panel A shows the ICM slot blot for a single DNA concentration of 3 μg. Panel B shows the digitized data where the ICM signal was arbitrarily assigned unit values based upon phosphorimaging of a single DNA concentration on the ICM slot blot.

covalent intermediate is transient and quickly resolves as the enzyme turns over; however, when aza-dC has been inserted into the DNA, this interaction results in the formation of an irreversible protein-genomic DNA complex. The catalytic center of DNMT becomes covalently bound to the 6 position of the cytosine ring (9, 15, 33, 34). Thus, in order to trap DNMT on the genome in vivo, aza-dC must be present. DNMT is presumably a typical DNA binding protein and will be in either a linear search mode over DNA or weakly bound in a complex with DNA and other ligands in chromatin. Upon making contact and gaining access to the aza-dC target site, DNMT-DNA complexes form that resist dissociation with protein denaturants, and these adducts do not readily reverse. With regard to the ICM technique described here, ionic detergents arrest the enzyme activity and at the same time disrupt the bulk of electrostatic protein-DNA complexes in the cell. DNA is then purified (without proteases) by CsCl gradient centrifugation, which completely dissociates noncovalent protein-DNA interactions and gives complete resolution of DNA from free protein with a recovery of 95 to 100%. This DNA is highly purified and free of bulk chromosomal proteins (such as histones) and has not been treated with proteases or phenol. An antibody probe is then used to quantify DNMT levels in the DNA fraction from the gradient. Several points should be stressed about the use and application of this technology. The method gives a snapshot of DNMT activity on the genome of any given cell or tissue that represents the physical interactions between DNMT and genomic DNA at the time of cell lysis. By analogy to well-characterized prokaryotic methyltransferases, aza-dC is a necessary in order to drive adduct formation (6). The fact that methylation can be also detected at aza-dC sites (6, 10) is mutually consistent with the notion that ICM detection of aza-dC DNA-DNMT adducts represents bona fide methylation sites. The method is quantitative and can be used with virtually any cell or tissue as long as the genome can be prelabeled with aza-dC. Since the ICM relies on monospecific antibody probes, it is highly specific for a given DNMT isoform and provides insight on the behavior of a given DNMT in vivo. For example, DNMT1 is strongly S phase dependent, based on the ICM (M. T. Muller and Y. F. Wang, unpublished data);

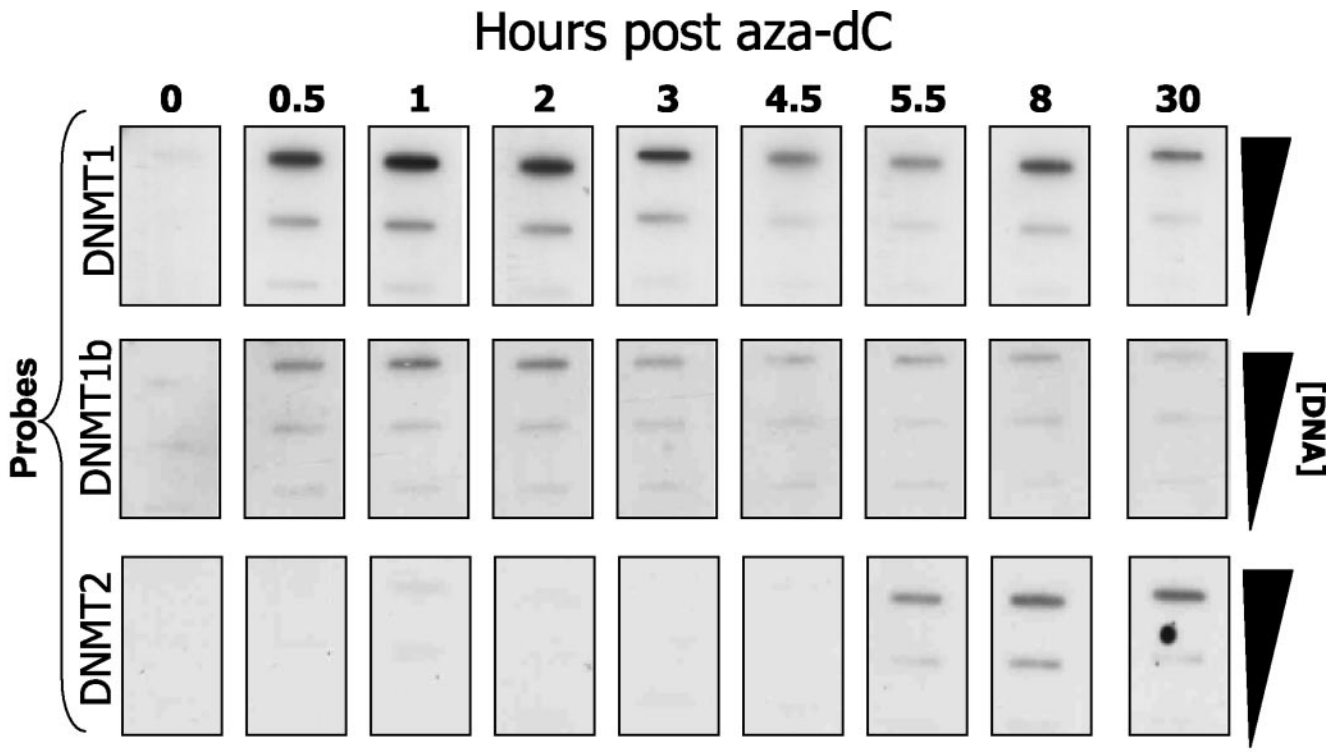

FIG. 5. Comparative analysis of DNMT1, DNMT1b, and DNMT2 in HeLa cells. HeLa cells in exponential growth (4×10^7/ICM assay) were treated with 5 μM aza-dC for the times indicated ("0" corresponds to a negative control) and were subjected to the ICM analysis by using two different probes: anti-DNMT1 (top row) and anti-DNMT1b (middle row) and anti-DNMT2 antibody (bottom). The amount (in micrograms) of DNA loaded per slot is indicated on the right side of the blot.

therefore, the assay is most likely detecting events at DNA replication forks or very soon after nascent DNA synthesis.

The following pieces of evidence attest to the validity of the ICM method for quantifying DNMT-DNA interactions in vivo.

(i) We note that there is a total dependence on preincorporation of aza-dC. That dependence, based upon collective data from a number of different labs (6, 9, 10, 15, 33, 34), suggests that catalytically active methylases are being detected.

(ii) Western blotting experiments demonstrate that DNMT polypeptide bands are depleted by aza-dC treatment. The loss of the signal is due to adduct formation on genomic DNA, which renders the trapped DNMT nonextractable. When tested, band depletion is always attended by an increase in DNMT in the DNA peak fraction of a CsCl gradient. Neither band depletion nor adducts were seen in HCT-116 *Dnmt1*$^{-/-}$ deletion mutants (27) (with a DNMT1 antibody probe). The band depletion data also reveal the overall efficiency of complex formation. Any reduction in the amount of total polypeptide should be directly proportional to the number of enzyme molecules stably bound to the genome. The efficiency is quite high (>75%) for the maintenance enzyme DNMT1, which is the predominant activity in cells. In contrast, murine DNMT2, -3a, and -3b band depletions were much less obvious and probably no more than 10%. While all of these were detected by ICM assay, the low efficiency may reflect the low relative activity (or high DNA sequence selectivity in chromatin) of these isoforms relative to maintenance methylation; however, additional data will be required to confirm this. It is safe to say that our present data show that all of these isoforms stably and selectively bind aza-dC- substituted DNA in vivo. These data suggest that, in mouse P19 cells, DNMT2, -3a, and -3b are active and that DNMT3b displays higher ICM activity than does DNMT2 or -3a. In human and mouse cells tested, DNMT2 binding to genomic DNA was clearly detectable but was also consistently lower than for other isoforms.

(iii) The ICM method does not detect other covalently bound proteins that associate with genomic DNA. Genomic DNA from cells treated with topoisomerase poisons (that are known to induce topoisomerase adducts) does not contain detectable DNMT. It is very unlikely that our DNMT antibodies are detecting nonmethylase proteins that may be stably bound to the genome. In contrast, treating with topoisomerase poisons plus aza-dC gives strong signals for both classes of covalent DNA binding proteins. The finding that topo I complexes are enhanced by aza-dC supports the notion that DNA-DNMT1 complexes are sites of DNA damage and that topo I is being recruited to these regions to assist in repair or recombination to remove the lesions (20, 32, 37).

(iv) The ICM complexes recovered from CsCl gradients were found to contain a DNMT1 polypeptide with a small DNA fragment following extensive digestion with DNase I. Essentially all of the DNMT1 was electrophoretically shifted due to the single-stranded nucleic acid tail that was covalently bound. This result shows that all of the DNMT1 found in the DNA peak is stably (covalently) bound to nucleic acid. We

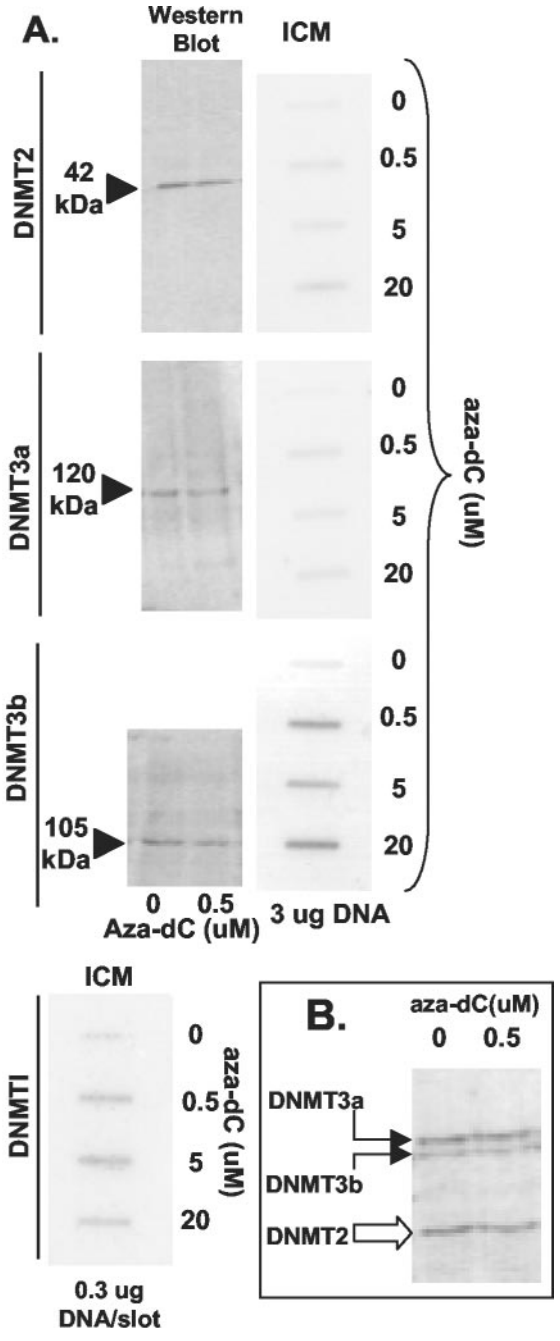

FIG. 6. Comparing endogenous DNMTs in mouse cells. (A) P19 cell cultures in exponential growth (4×10^7/dish) were treated with 0, 0.5, 5, or 20 μM aza-dC for 8 h. Half of the cultures were subjected to the ICM analysis (slot blots labeled ICM on top) by using anti-DNMT probes indicated on the left. Nuclear extracts were prepared (from duplicate cultures) and were analyzed by SDS-polyacrylamide gel electrophoresis and Western blotting by using the probes shown on the left. For the Western blots (150 μg of protein per lane) only the 0 and 0.5 μM aza-dC samples are shown. For the ICM analysis, all concentrations of aza-dC titration are shown, with use of a fixed amount of DNA in each slot (3 or 0.3 μg as indicated). (B) An admixture of antibodies was used for two P19 nuclear extracts (150 μg/lane) prepared from cells treated with 0 or 0.5 μM aza-dC (8 h).

estimate that 20 to 30 nucleotides remained; however, accurate estimates in this size range (>200 kDa) are crude at best.

The ICM method is antibody based and can be used to biochemically track different DNMT isoforms that engage an aza-dC-labeled genome. We show that in fact the DNMT1b variant is quite an active DNA methylase in vivo and mirrors the action of the more abundant DNMT1 activity (DNMT1b complexes being roughly 10% of DNMT1). This ratio is close to that predicted by mRNA expression analysis (13) but is higher than expected based upon Western blotting data (5). While total DNMT1b may be low, it can bind efficiently to aza-dC-substituted genomic DNA, suggesting robust methylation activity in vivo. Our collective data show that the DNA-hypomethylating drug aza-dC has multiple targets in vivo. In double knockouts of *Dnmt1* and *Dnmt3b* (28), the DNMT1b splice variant would also be absent; however, based upon the ICM, this variant may contribute to the global methylation patterns in vivo in wild type cells. Understanding isoform-specific methylation in vivo is further complicated by studies showing the existence of multiple isoforms of DNMT3b, some of which are inactive in vitro (1). In our present study, we could not examine different DNMT3b isoforms due to the lack of specific antisera; however, the ICM has the potential to resolve these issues in a biologically relevant context.

The availability of monospecific mouse antibodies allowed us to compare several DNMT isoforms in the murine system. Our data show that DNMT1, -3a, -3b, and -2 stably and specifically bind aza-dC-substituted genomes, suggesting that these are all active transmethylases in mouse P19 embryonic carcinoma cells (Fig. 6). Based upon the ICM assay, it appears that, after 8 h of aza-dC treatment, DNMT3b displayed considerably higher (four- to fivefold) global activity than did DNMT2 and -3a; however, DNMT3b expression was about half the levels of DNMT3a and DNMT2. A possible explanation is that the endogenous catalytic activity of each DNMT is regulated by other proteins or by accessibility of a DNA target in chromatin (recently reviewed in reference 29). For example, DNMT3b colocalizes to pericentromeric heterochromatin, which, as a repetitive element, may represent a localized sink for DNMT3b activity. Alternatively, this may simply be a unique feature of embryonic carcinoma cells; however, recent results showing that DNMT3b works coordinately with DNMT1 in maintaining genomic methylation states (28) support the notion that DNMT3b and -1 are operating at higher levels in vivo.

In the two species tested (human and mouse), our data suggest that DNMT2 is a catalytically active transmethylase in a chromosomal setting. DNMT2 is extremely well conserved, and a homolog exists in *Drosophila melanogaster.* Moreover, it has recently been reported that the fly genome contains 5-methyl cytosine (11, 19); thus, it is logical to presume that a functional methylase exists, although none has been reported. Additional support for this idea comes from reports that aza-dC is cytotoxic in *D. melanogaster* (17). As noted, DNMT2 is thus far the most highly conserved of all DNMTs containing key motifs found in other active methyltransferases (conserved proline-cysteine dipeptide active sites, for example). DNMT2 homologs have been found in plants, yeast, flies, mice, and humans (29); thus, given its evolutionary conservation, detecting catalytic activity in humans and mice might predict its

activity in the fruit fly. Clearly additional studies will be necessary to resolve these issues.

The time course of DNMT1-DNA complex formation following addition of aza-dC showed that DNMT1 adducts were consistently higher after short exposure to aza-dC and that, with time, the adduct formation decreased to a lower (but stable) level. A logical interpretation is that short drug exposures may saturate the genome with all active DNMT1; thus, adduct accumulation is maximum early. The subsequent reduction in total DNMT1-DNA adducts suggests two possibilities: first, we cannot rule out that aza-dC- treated cells are simply dying off due to cytotoxic consequences of the drug; however, we note that, under our experimental conditions (5 μM aza-dC), we did not detect an increase in dead cells (compared to negative controls) by flow cytometry in the first 24 h following drug addition (data not shown). After 24 h, we start to see a time-dependent increase in cell death and apoptosis. Second, the reduction in adducts might also suggest that they are healed or repaired. If this is the case, we conclude that these adducts are perceived and that sites of DNA damage (9, 15, 16) and cellular mechanisms exist to deal with DNMT1-DNA adduct formation. A precedent for cellular mechanisms that reverse covalent protein-DNA adducts has been reported in eukaryotes (14, 26, 40); therefore, it seems likely that enzymatic (or other) means exist to reverse (or repair) the DNMT1-DNA adducts. The finding that aza-dC stimulates recombination in the fruit fly (24, 25) further suggests that recombination repair may be the adduct reversal that we report here. These reversal pathways are of obvious importance to the application of hypomethylating drugs in the treatment of cancer. Further evaluation of the biological consequences of DNMT1 adducts in repair- proficient and -deficient cell lines is ongoing to examine this specific point (Wang and Muller, unpublished).

ACKNOWLEDGMENTS

We thank B. Vogelstein and S. Baylin (Johns Hopkins University) for generously providing the HCT-116 cell lines used in this study. We also thank Christoph Plass (Ohio State University) and Keith Robertson (National Cancer Institute) for helpful discussions, reagents, and input on this work and X. Cheng (Emory University) for providing an anti-DNMT2 antibody probe.

REFERENCES

1. **Aoki, A., I. Suetake, J. Miyagawa, T. Fujio, T. Chijiwa, H. Sasaki, and S. Tajima.** 2001. Enzymatic properties of de novo type mouse DNA (cytosine-5) methyltransferases. Nucleic Acids Res. **29:**3506–3512.
2. **Baylin, S. B., M. Esteller, M. R. Rountree, K. E. Bachman, K. Schuebel and J. G. Herman.** 2001. Aberrant patterns of DNA methylation, chromatin formation and gene expression in cancer. Hum. Mol. Genet. **10:**687–692.
3. **Belinsky, S. A., K. J. Nikula, W. A. Palmisano, R. Michels, G. Saccomanno, E. Gabrielson, S. B. Baylin, and J. G. Herman.** 1998. Aberrant methylation of p16INK4a is an early event in lung cancer and a potential biomarker for early diagnosis. Proc. Natl. Acad. Sci. USA **95:**11891–11896.
4. **Bestor, T.** 2000. The DNA methyltransferases of mammals. Hum. Mol. Genet. **9:**2395–2402.
5. **Bonfils, C., N. Beaulieu, E. Chan, J. Cotton-Montpetit, and A. R. MacLeod.** 2000. Characterization of the human DNA methyltransferase splice variant Dnmt1b. J. Biol. Chem. **275:**10754–10760.
6. **Brank, A. S., R. Eritja, R. G. Barcia, V. E. Marquez, and J. K. Christman.** 2002. Inhibition of HhaI DNA (Cytosine-C5) methyltransferase by oligodeoxyribonucleotides containing 5-aza-2′-deoxycytidine: examination of the intertwined roles of co-factor, target, transition state structure and enzyme conformation. J. Mol. Biol. **323:**53–67.
7. **Costello, J. F., and C. Plass.** 2001. Methylation matters. J. Med. Genet. **38:**285–303.
8. **Dong, A. Y., J. A. Yoder, A. Zhang, L. Zhou, T. H. Bestor, and X. Cheng.** 2001. Structure of human DNMT2, an enigmatic DNA methyltransferase homolog that displays denaturant-resistant binding to DNA. Nucleic Acids Res. **29:**439–448.
9. **Ferguson, A., P. Vertino, J. Spitzner, S. Baylin, M. Muller, and N. Davidson.** 1997. Role of estrogen receptor gene demethylation and DNA methyltransferase-DNA adduct formation in 5′-aza-2′ deoxycytidine-induced cytoxicity in human breast cancer cells. J. Biol. Chem. **272:**32260–32266.
10. **Gabbara, S., and A. S. Bhagwat.** 1995. The mechanism of inhibition of DNA (cytosine-5-)-methyltransferase by 5-azacytosine is likely to involve methyl transfer to the inhibitor. Biochem. J. **307:**87–92.
11. **Gowher, H., O. Leismann, and A. Jeltsch.** 2000. DNA of Drosophila melanogaster contains 5-methylcytosine. EMBO J. **19:**6918–6923.
12. **Hsieh, C.-L.** 1999. In vivo activity of murine de novo methyltransferases, Dnmt3a and Dnmt3b. Mol. Cell. Biol. **19:**8211–8218.
13. **Hsu, D.-W., M.-J. Lin, T.-L. Lee, S.-C. Wen, X. Chen, and C.-K. J. Shen.** 1999. Two major forms of DNA (cytosine-5) methyltransferase in human somatic tissues. Proc. Natl. Acad. Sci. USA **96:**9751–9756.
14. **Interthal, H., J. J. Pouliot, and J. J. Champoux.** 2001. The tyrosyl-DNA phosphodiesterase Tdp 1 is a member of the phospholipase D superfamily. Proc. Natl. Acad. Sci. USA **98:**12009–12014.
15. **Juttermann, R., E. Li, and R. Jaenisch.** 1994. Toxicity of 5-aza-2′-deoxycytidine to mammalian cells is mediated primarily by covalent trapping of DNA methyltransferase rather than DNA demethylation. Proc. Natl. Acad. Sci. USA **91:**11797–11801.
16. **Karpf, A. R., B. C. Moore, T. O. Ririe, and D. A. Jones.** 2001. Activation of the p53 DNA damage response pathway after inhibition of DNA methyltransferase by 5-aza-2′-deoxycytidine. Mol. Pharmacol. **59:**751–757.
17. **Katz, A. J.** 1985. Genotoxicity of 5-azacytidine in somatic cells of Drosophila. Mutat. Res. **143:**195–199.
18. **Li, E., T. Bestor, and R. Jaenisch.** 1992. Targeted mutation of the DNA methyltransferase gene results in embryonic lethality. Cell **69:**915–926.
19. **Lyko, F., B. H. Ramsahoye, and R. Jaenisch.** 2000. DNA methylation in Drosophila melanogaster. Nature **408:**538–540.
20. **Mao, Y., S. Okada, L. Chang, and M. T. Muller.** 2000. p53 dependence of topoisomerase I recruitment *in vivo*. Cancer Res. **60:**4538–4543.
21. **Okano, M., D. Bell, D. Haber, and E. Li.** 1999. DNA methyltransferases Dnmt3a and Dnmt3b are essential for de novo methylation and mammalian development. Cell **99:**247–257.
22. **Okano, M., S. Xie, and E. Li.** 1998. Dnmt2 is not required for de novo and maintenance methylation of viral DNA in ES cells. Nucleic Acids Res. **26:**2536–2540.
23. **Ordway, J. M., and T. Curran.** 2002. Methylation matters: modeling a manageable genome. Cell Growth Differ. **13:**149–162.
24. **Osgood, C. J., and S. M. Seward.** 1989. 5-Azacytidine induces sex chromosome loss and interchange in immature germ cells of Drosophila mei-9 males. Environ. Mol. Mutag. **14:**135–145.
25. **Pontecorvo, G., A. Avitabile, G. Esposito, G. Migliaccio, and M. Carfagna.** 1992. Induced crossing-over in Drosophila melanogaster germ cells of DNA repair-proficient and repair-deficient (mei-9L1) males following larval feeding with 5-azacytidine and mitomycin C. Mutat. Res. **266:**93–98.
26. **Pouliot, J. J., K. C. Yao, C. A. Robertson, and H. A. Nash.** 1999. Yeast gene for a tyr-DNA phosphodiesterase that repairs topoisomerase I complexes. Science **286:**552–555.
27. **Rhee, I., K. Jair, R. Yen, C. Lengauer, J. Herman, K. Kinzler, B. Vogelstein, S. Baylin, and K. E. Schuebel.** 2001. CpG methylation is maintained in human cancer cells lacking DNMT1. Nature **404:**1003–1007.
28. **Rhee, I., K. E. Bachman, B. H. Park, K. W. Jair, R. W. Yen, K. E. Schuebel, H. Cui, A. P. Feinberg, C. Langeur, K. W. Kinzler, S. B. Baylin, and B. Vogelstein.** 2002. DNMT1 and DNMT3b cooperate to silence genes in human cancer cells. Nature **416:**552–556.
29. **Robertson, K. D.** 2002. DNA methylation and chromatin—unraveling the tangled web. Oncogene **21:**5361–5379.
30. **Robertson, K. D.** 2001. DNA methylation, methyltransferases, and cancer. Oncogene **20:**3139–3155.
31. **Robertson, K., et al.** 1999. The human DNA methyltransferases (DNMTs) 1, 3a and 3b: coordinate mRNA expression in normal tissues and overexpression in tumors. Nucleic Acids Res. **27:**2291–2298.
32. **Rosenstein, B. S., D. Subramanian, and M. T. Muller.** 1997. The involvement of topoisomerase I in the induction of DNA-protein crosslinks and DNA single-strand breaks in cells of ultraviolet-irradiated human and frog cell lines. Radiat. Res. **148:**575–579.
33. **Santi, D., C. E. Garrett, and P. J. Barr.** 1983. On the mechanism of inhibition of DNA-cytosine methyltransferases by cytosine analogs. Cell **33:**9–15.
34. **Santi, D. V., A. Normant, and C. E. Garrett.** 1984. Covalent bond formation between a DNA-cytosine methyltransferase and DNA containing 5-azacytosine. Proc. Natl. Acad. Sci. USA **81:**6993–6997.
35. **Subramanian, D., E. Kraut, A. Staubus, D. Young, and M. T. Muller.** 1995. Analysis of topoisomerase I complexes in patients being treated with topotecan. Cancer Res. **55:**2097–2103.
36. **Subramanian, D., C. Sommer Furbee, and M. T. Muller.** 2000. ICE bioassay. Isolating in vivo complexes of enzyme to DNA. Methods Mol. Biol. **95:**137–147.
37. **Subramanian, D., B. Rosenstein, and M. T. Muller.** 1998. Ultraviolet-in-

duced DNA damage stimulates topoisomerase I-DNA complex formation in vivo: possible relationship with DNA repair. Cancer Res. **58:**976–984.

38. **Trask, D. K., J. A. DiDonato, and M. T. Muller.** 1984. Rapid detection and isolation of covalent DNA/protein complexes: application to topoisomerase I and II. EMBO J. **3:**671–676.
39. **Trask, D. K., and M. T. Muller.** 1988. Stabilization of type I topoisomerase-DNA covalent complexes by actinomycin D. Proc. Natl. Acad. Sci. USA **85:**1417–1421.
40. **Yang, S., A. B. Burgin, B. N. Huizenga, C. A. Robertson, K. C. Yao, and H. A. Nash.** 1996. A eukaryotic enzyme that can disjoin dead-end covalent complexes between DNA and type I topoisomerases. Proc. Natl. Acad. Sci. USA **93:**11534–11539.